Experimental study of the interaction between terahertz radiation from the Novosibirsk free-electron laser and water aerosol

G. Kulipanov, A. Lisenko, G. Matvienko, V. Oshlakov, S. Babchenko

G. N. Kulipanov, A. A. Lisenko, G. G. Matvienko, V. K. Oshlakov, S. V. Babchenko, "Experimental study of the interaction between terahertz radiation from the Novosibirsk free-electron laser and water aerosol," Proc. SPIE 9292, 20th International Symposium on Atmospheric and Ocean Optics: Atmospheric Physics, 92922J (25 November 2014); doi: 10.1117/12.2075004

SPIE.

Event: 20th International Symposium on Atmospheric and Ocean Optics: Atmospheric Physics, 2014, Novosibirsk, Russian Federation

Experimental study of the interaction between terahertz radiation from the Novosibirsk free-electron laser and water aerosol

G.N. Kulipanov[1], A.A. Lisenko[2,3], G.G. Matvienko[2,3], V.K. Oshlakov[2], S.V. Babchenko[2]
[1]*Institute of Nuclear Physics SB RAS, Novosibirsk, e-mail: G.N.Kulipanov@inp.nsk.su*
[2]*V.V. Zuev Institute of Atmospheric Optics SB RAS, Tomsk, e-mail: Lisenko@iao.ru*
[3]*Tomsk State University, Tomsk, e-mail: Lisenko@iao.ru*

ABSTRACT

The interaction of high-power terahertz radiation from the Novosibirsk free-electron laser at a wavelength of 130 μm in atmospheric transparency window with a model aerosol cloud having the known droplet size distribution function has been studied experimentally for the first time. The experimental data are compared with theoretical calculations obtained from solution of the lidar equation for conditions of the experiment.

Key words: Novosibirsk free-electron laser, lidar equation, aerosol cloud

1. INTRODUCTION

Nowadays, the significant progress in the field of generation and detection of terahertz radiation (0.3-10 THz corresponds to λ = 1 mm-30 μm) has led to the intense development of systems for remote monitoring of the atmosphere. New-generation millimeter and submillimeter radiometers for spaceborne systems have been developed to monitor the phase composition of stratospheric crystal clouds and associated radiative processes; these systems are capable of operating at frequencies up to 3 THz [1, 2]. This wide frequency coverage allows the high sensitivity to be provided for a wide size range of cloud particles, because the radiation wavelength in the THz range becomes comparable with diameters of large cloud particles [3,4].

The remote sensing of the lower atmosphere, which is inaccessible for satellite measurements, in order to study peculiarities of the spatiotemporal variability of atmospheric water content, phase composition of low-level clouds, fog, and precipitation, as well as other problems, also requires the extension of the frequency range of active remote sensing facilities. It should be noted that there are practically no sources of THz range suitable for active remote sensing, and therefore the interest of specialists in lidar sensing of environment to the Novosibirsk free-electron laser (FEL) is evident. First, the pulse and average spectral power of radiation of this laser is record in the world and will likely remain record in the nearest future (P_{pulse} ~ 1 MW, P_{av} ~ 0.5 kW) [5]. No one of currently available sources of THz radiation has power sufficient for solution of the mentioned problems in the lower atmosphere. Second, the wide range of continuous frequency tuning of FEL allows implementation of the technique of multifrequency sensing of microphysical parameters of aerosol particles, because there is the possibility of selecting the sensing wavelengths in atmospheric transparency windows in the entire FEL range from 7 to 235 μm, and these wavelengths can be informative for a wide range of problems of remote atmospheric sensing. If the range 7–30 μm, corresponding to the 3-rd stage of FEL, is studied rather well, then in the range 30–235 μm there exist some problems connected with the absence of experimental studies of both the atmospheric transmittance and the interaction of THz radiation with the water aerosol.

Theoretically, the interaction of THz radiation with the water liquid droplet aerosol is studied quite thoroughly now, but is not confirmed experimentally yet. The aim of our experimental study is to fill this gap.

2. EXPERIMENT

To conduct an experiment on the interaction of THz radiation with the liquid droplet water aerosol, we have assembled a test bench including the following elements: radiation source (FEL), optomechanical modulator, Newtonian telescope, receiver of radiation, electronic unit for digital data acquisition and processing. The block diagram of the experiment is shown in Fig. 1.

20th International Symposium on Atmospheric and Ocean Optics: Atmospheric Physics, edited by Gennadii G. Matvienko, Oleg A. Romanovskii, Proc. of SPIE Vol. 9292, 92922J · © 2014 SPIE · CCC code: 0277-786X/14/$18 · doi: 10.1117/12.2075004

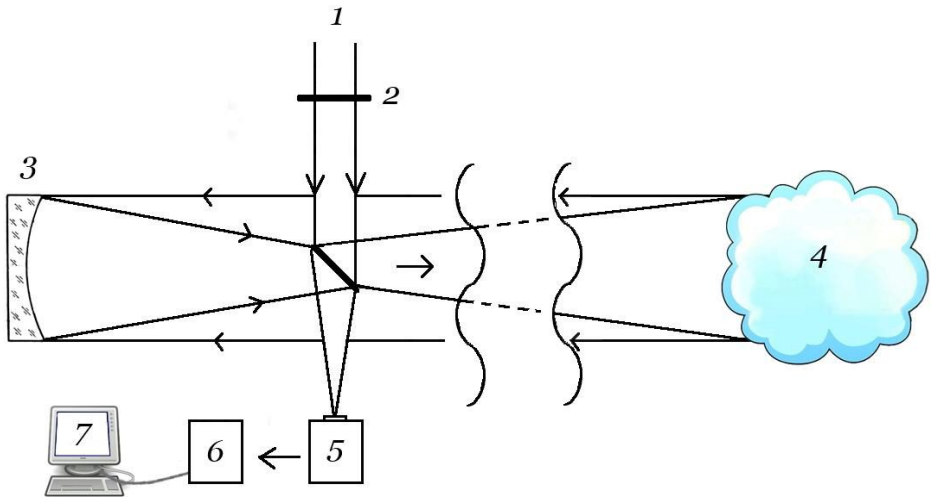

Fig. 1. Block diagram of experiment: 1 – FEL radiation, 2 – optomechanical modulator, 3 – Newtonian telescope, 4 – aerosol cloud, 5 – receiver of radiation, 6 – electronic module for digital data acquisition, 7 - computer.

The FEL radiation at a wavelength of 130 μm had the following parameters: degree of linear polarization я > 99.6 %, radiation diffraction divergence of beam $\theta = 4.3$ mrad, beam diameter r_0=1.62 cm, pulse repetition frequency f = 10 MHz, average power P_{av}=100 W, pulse duration $\tau = 100$ ps, P_{pulse}=0.1 MW. The spectrum of radiation in the atmospheric transparency window recorded by BRUKER IFS 66 v/s is shown in Fig. 2. The transmittance of the atmospheric window T was calculated from the data of JPL Submillimeter Catalog, which contains the information about 916 lines of water molecule in the ground vibrational state and 55983 absorption lines of vibrationally excited water molecules, for a distance of 10 m at the specific content of water vapor w = 0.12 cm/km.

The backscattered signal was detected with the Tydex GC-1P optoacoustic detector (Golay cell) [6] falling in the class of nonselective uncooled detectors capable of recording low-energy signals up to 10^{-5} J in the wavelength region from 0.3 μm to 6-8 mm. The main feature of this detector is the necessary use of a modulator interrupting the radiation flux. The choice of the working frequency (f_r = 17 Hz) was caused by the peculiarity of operation of the optoacoustic detector and connected, first of all, with the fact that the optimal frequency range, where the detector has the highest sensitivity, is the range 10-25 Hz. At the modulation frequency of 17 Hz and the exit window diameter d = 5 mm, the GC-1P optoacoustic detector has the following main characteristics: optical sensitivity $W=8.7\times10^4$ V/W, noise equivalent power $NEP=1.1\times10^{-10}$ W/Hz$^{1/2}$, response time t=36 mc, detectivity $D^*=3.9\times10^9$ cm Hz$^{1/2}$/W. The detectivity characterizes the signal-to-noise ratio (S/N) at the incidence of radiation with 1-W power onto the receiving aperture and is calculated as:

$$D^* = \left(S/N \times \sqrt{\Delta f}\right) \Big/ \left(P \times \sqrt{A}\right) \quad (1)$$

where S is the detector output signal, N is the detector noise, P is the detector input power, A is the area of the receiving aperture [cm^2], Δf is the width of the noise band [Hz]. The noise equivalent power NEP is determined as

$$NEP = \sqrt{A}/D^* \ \ (\mathrm{W/hz^{1/2}})$$

The experiment essentially consisted in the recording of radiation modulated by the optomechanical modulator and scattered by an aerosol cloud at a short, up to 10 m, path. The scattered radiation was collected by the Newtonian telescope with the mirror area S_r=0.07 m^2 and focused onto the input of the optoacoustic detector. The signal from the sensor came to the electronic module for digital acquisition and processing of data.

Figure 3 shows an example of the recorded signal backscattered from an aerosol cloud at a distance of 3 m. The plot is the FFT (Fast Fourier Transform) spectrum of the input signal. The frequency is platted as the horizontal axis, while the vertical axis is the spectral density of the input signal measured in RMS (root mean square) volts and connected with the square root of the frequency band width, in Hz. The peak of the backscattered signal with amplitude of 0.0058 V falls at a frequency of 17 Hz. Known the optical sensitivity of the detector, we can calculate the value of P_s and determine S/N from Eq. (1). For this case S/N =8. In the experiment, we have also detected noise signals of thermal background at frequencies multiple of 50 Hz, whose origin is explained by operation of the devices in the power supply line with a

frequency of 50 Hz, and at other frequencies, which are connected with mechanical oscillations falling within the detector sensitivity range.

3. MATHEMATICAL SIMULATION

For simulation of the experiment, we estimate the S/N ratio given the FEL radiation parameters, optical arrangement of detection, characteristics of the GC-1P optoacoustic detector, and optical characteristics of the model aerosol cloud and the atmosphere. The value of S/N can be estimated from the equation [7,8]:

$$S/N = \frac{P_s}{\sqrt{2\Delta f\,(P_s+P_b)\frac{2hc}{\lambda\eta} + NEP^2\Delta f}} \tag{2}$$

The power of the lidar echo signal from the aerosol cloud P_s can be determined as

$$P_s = P_0 \cdot \frac{c\tau}{2} K(r) \cdot G(r) \cdot \beta_\pi(r) \cdot \left(\frac{S_r}{r^2}\right) \cdot T_a^{\,2} \tag{3}$$

where P_0 is the FEL peak power, K(r) is the instrumental constant, c is the speed of light, τ is the pulse duration, S_r is the area of the receiving antenna, G(r) is the geometric factor, β_π(r) is the volume backscattering coefficient in the unit

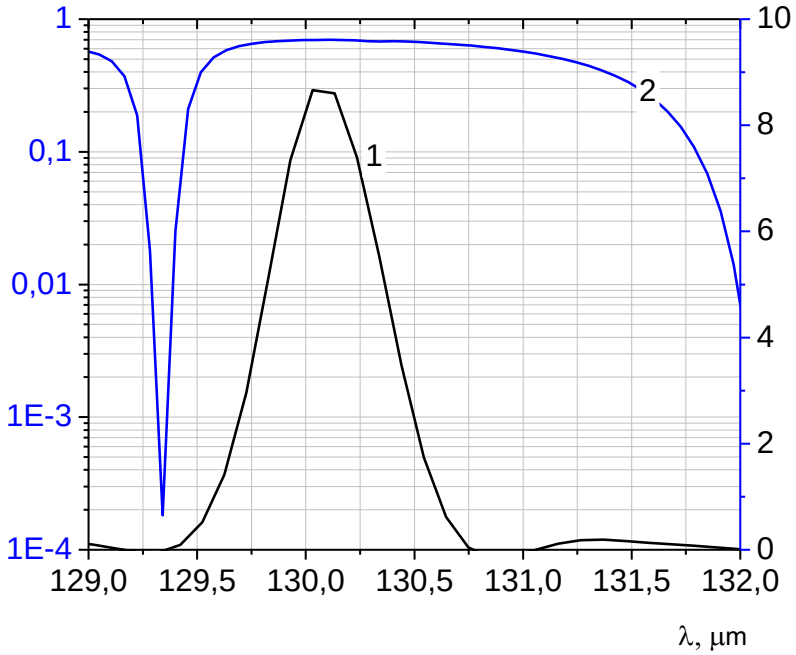

Fig 2. Spectrum of radiation of Novosibirsk FEL at a wavelength of 130 μm (curve 1) in the atmospheric transparency window as calculated for a distance of 10 m at the specific water vapor content w = 0.12 cm/km (curve 2).

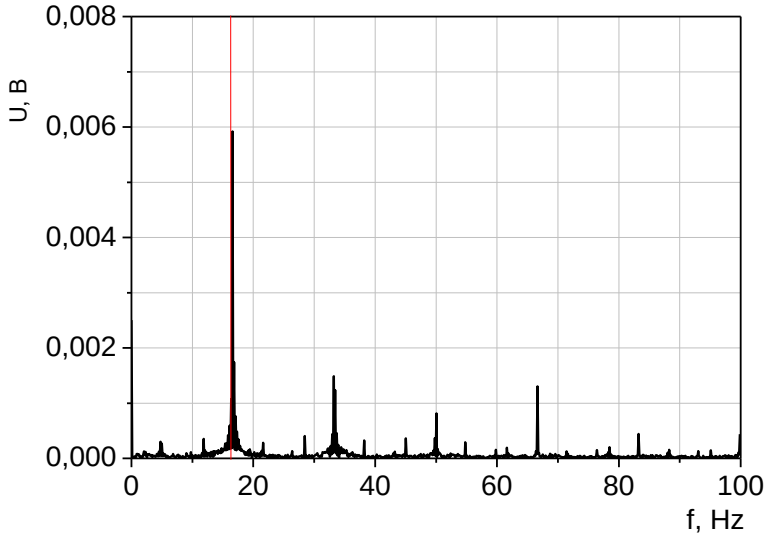

Fig. 3 Backscattered signal recorded by the GC-1P optoacoustic detector at a modulation frequency of 17 Hz from a cloud of liquid droplet water aerosol. Neighboring peaks correspond to the external thermal background modulated by frequencies multiple to 50 Hz (frequency of the power supply line).

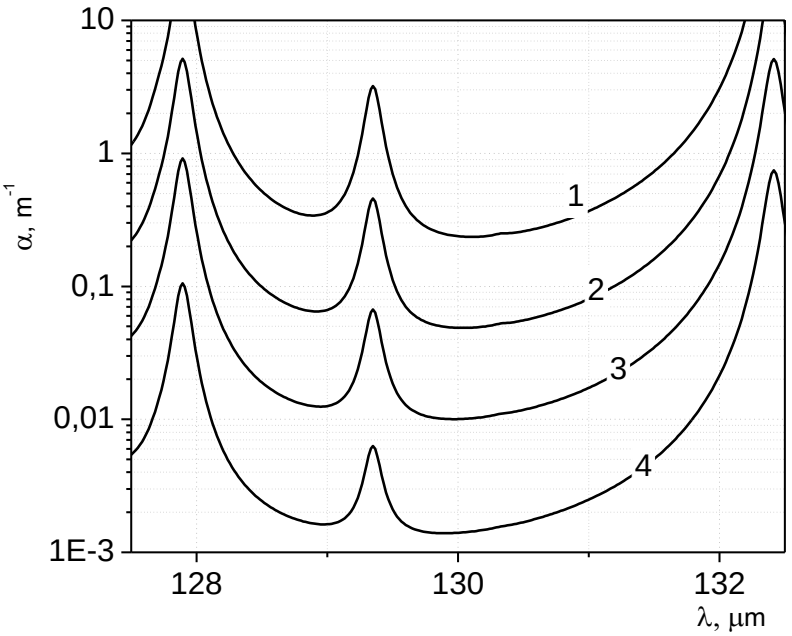

Fig.4 Absorption in the atmospheric transparency window centered at 130 μm at different values of the specific water vapor content: (curve 1) w_1= 0.6 cm/km, (curve 2) w_2= 1.2 cm/km, (curve 3) w_3= 0.02 cm/km, and (curve 4) w_4= 0.03 cm/km (cm/km).

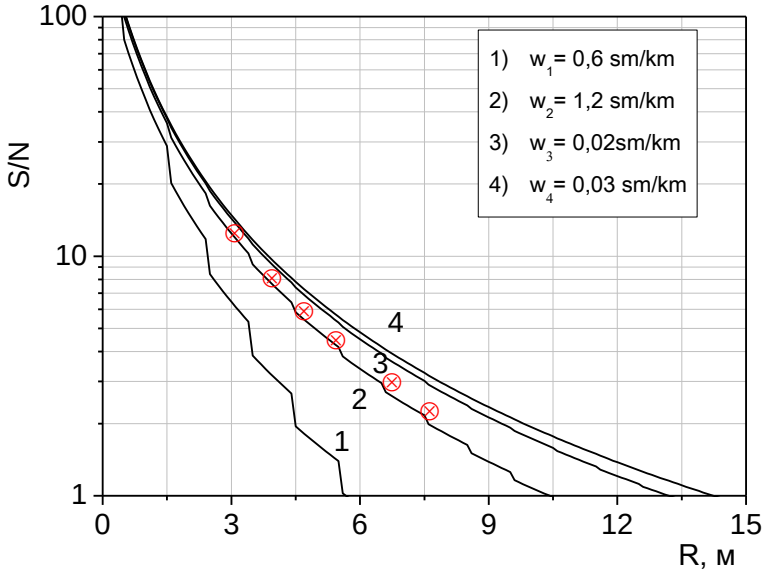

Fig.5. Comparison of experimental and calculated values of S/N at a wavelength of 130 μm.

solid angle, T_a is transmittance of the atmosphere and the aerosol cloud. At this wavelength, T_a obeys the Bouguer—Lambert—Beer law

$$T_a = \exp\left(\int_0^R -\left[\gamma_m(\lambda,r)+\gamma_a(\lambda,r)\right]dr\right), \quad (4)$$

where r is distance, γ_m and γ_a are the coefficients of radiation extinction by the atmosphere and the aerosol cloud.
In the numerical experiment, the variation of molecular absorption by atmospheric water vapor is an input parameter in addition to the FEL radiation and detector parameters. Molecular scattering obeying the λ^{-4} law does not play a significant role in the THz range and can be neglected. The absorption coefficients α in the atmospheric transmission band cantered at a wavelength of 130 μm for different values of the specific water vapor content w are shown in Fig. 4. The scattering at the cloud of liquid droplet water aerosol is explained by the Mie theory, which is valid for both the scattering at large particles, whose size is comparable with or much larger than the radiation wavelength, and the scattering at small particles, whose size is much smaller than the wavelength. For the calculation of the optical coefficients of interaction of the FEL radiation at λ=130 μm with the aerosol cloud, we have selected the cloud model described by the lognormal droplet size distribution with a modal radius of 2 μm. The calculations by the Mie theory yielded the following values of the optical interaction coefficients, which were then used in the following calculations: extinction coefficient γ_a=1.31e-6 m^{-1}, backscattering coefficient β_π = 1.03e-8 m^{-1}.
Figure 5 depicts calculated S/N (black solid curves) for the different content of water vapor at the sensing path, and the red circles show experimental values of S/N obtained from measurements with different distances to the aerosol cloud. The measurements are in good agreement with the curve corresponding to the water vapor content of 0.12 cm/km, which is close to the actual conditions of the experiment.

4. CONCLUSIONS

The results of the experiment and numerical simulation of detection of the signal backscattered from an aerosol cloud with the modal droplet radius of 2 μm at a wavelength of 130 μm have demonstrated the good qualitative agreement.

This indicates that we can expect an increase of the backscattering signal by orders of magnitude if an aerosol cloud contents particles, whose size is comparable with the radiation wavelength, but the experiment should be continued.

REFERENCES

[1] Siegel, P.H. "THz Instruments for Space", IEEE. Transactions on Antennas and Propagation. 55(11), 2957-2965 (2007).

[2] Racette, P., Adler, R.F., Wang, J.R., Gasiewski, A.J., Jackson, D.M.and Zacharias, D.S. "An airborne millimeter-wave imaging radiometer for cloud, precipitation, and atmospheric water vapor studies", Appl. Oceanic Technol. 13. 610–619 (1996).

[3] Wu, D. L., Pickett, H. M. and Livesey, N. J. "Aura MLS THz observations of global cirrus near the tropopause", Geophysical Research Letters 35 (L15803) doi:10.1029/2008GL034233, (2008).

[4] Mendrok, J., Baron, P., and Kasai, Y. "Studying the Potential of Terahertz Radiation for Deriving Ice Cloud Microphysical Information", Remote Sensing of Clouds and the Atmosphere XIII, Proc. of SPIE 7107,710704 doi:10.1117/12.800262.

[5] Knyazev, B.A., Kulipanov, G.N., Vinokurov, N.A. "Novosibirsk terahertz free electron laser: instrumentation development and experimental achievements", Measurement Science and Technology, 21(054017) (2010).

[6] http://www.tydex.ru

[7] Measures, R.M., "Laser Remote Sensing. Fundamentals and Applications", John Wiley & Sons, (1984).

[8] Ivashchenko, M.V., Sherstov, I.V. "Range of differential-absorption lidar based on CO_2 laser", Quantum Electronics, 30(8), 747-752 (2000).